Design of an Hybrid Battery/Super-capacitors Energy Storage System for Hybrid Electric Vehicles

Hayet Slimani Khaldi[1], Ahmed Chiheb Ammari[1,2]

[1.] Matériaux, Mesures et Application (MMA) Laboratory, INSAT Institute Carthage University, Tunis, Tunisia
[2.] Department of Electrical & Computer Engineering, Faculty of Engineering King Abdulaziz University, Jeddah, Saudi Arabia
hayet.slimani@gmail.com

Abstract: Hybrid Energy Storage Systems (HESS) used for Electric Vehicles (EV) and Hybrid Electric Vehicles (HEV) are capable for achieving superior storage performances to that of any of its single storage components. This paper presents the design of an HESS that enables for the desired performance characteristics of an HEV in terms of power and energy requirements. The HESS is composed with Lithium-ion battery and super-capacitors packs. Each single storage element is connected via a particular DC/DC power converter to a common DC-link. The design aims to find the optimal parameters of the different devices according to a proposed set of specifications. A comparison between two DC/DC converter topologies interfacing the HESS to the DC link is also performed. The studied topologies concern classic and Three Level (TL) DC/DC boost and buck/boost converters. The obtained results show that the TL converters enables for a reduced cost, weight and volume and allows for the best utilization of battery and super-capacitor technologies for both high energy and high power densities. Matlab/Simulink models of battery, super-capacitors and of the different DC/DC converter topologies are developed. The system behaviour and performance results are obtained and discussed.
[Hayet Slimani Khaldi, Ahmed Chiheb Ammari. **Design of an Hybrid Battery/Super-capacitors Energy Storage System for Hybrid Electric Vehicles.** *Life Sci J* 2014;11(12):109-118]. (ISSN:1097-8135). http://www.lifesciencesite.com. 18

Keywords: Lithium-ion battery; super-capacitor; DC/DC converter topologies; system sizing; energy storage

1. Introduction

The transportation field, one of the largest energy sectors, is currently facing pressing problems associated with the increasing air pollution, petroleum dependence, Green House Gases (GHG) emissions and other energy efficiency concerns. To address such problems and meet nowadays new challenges, Electric Vehicles (EV) and Hybrid Electric Vehicles (HEV) are considered to be interesting alternatives. In this context, one of the key issues related to the development of EV and HEV is the Energy Storage System (ESS) that has to satisfy all demands of the vehicle in terms of power and energy densities, cost and weight per unit capacity, round-trip efficiency, cycle life, and other environmental effects (Li et al., 2009). However, there is currently no single ESS element that can fulfil all the cost and performance storage requirements. Improving the performance of ESS systems can be achieved using different types of ESS elements, where each type has its unique strengths and weaknesses. An hybrid ESS (HESS) system can hide the drawbacks of a single type of ESS while implementing their benefits.

HESS has been an interesting research area for a long time (Lukic et al., 2008), (Baisden and Emadi, 2004), (Cao et al., 2007) and several studies have already been focused on HESS and their topologies over the past years (Lukic et al., 2008), (Kohler et al., 2009), (Hoelscher et al., 2006). The battery/super-capacitor configuration was the most studied HESS with many possible topologies connecting the two storage devices with the DC bus (Kohler et al., 2009), (Hoelscher et al., 2006), (Miller et al., 2009), (Cao and Emadi, 2009), (Li et al., 2004), (Li et al., 2009). All of these topologies have similar performance, but the design of the power converters and the choice of the energy sources (battery and super-capacitors) can be different from one topology to another. Usually, batteries are designed to provide the average power or steady-state power to the electric drive and super-capacitor will support for the peak power or transient power during acceleration and regenerative braking. The energy consumption of the vehicle is directly dependant on the size of the storage elements, the structure of the HESS and the strategy used for the power control.

In our study, the proposed HESS is sized to provide the same amount of energy and the same peak power as an equivalent single battery system. The present paper is concerned with the design of an HESS targeting a given electric vehicle system. Particularly, we are aiming to calculate the optimal sizing parameters of the different devices according to a proposed set of specifications and to obtain the optimal cost effective HESS that allows for the best utilization of battery and super-capacitor technologies for both high energy and high power densities. A

comparison between two DC/DC converter topologies interfacing the HESS (battery module and the super-capacitors module) to the DC link is also performed. The studied topologies concern a classic DC/DC boost and buck/boost converters and a Three Level (TL) boost and buck/boost converters.

This paper is organized as follows. Section 2 introduces the used topology for the HESS and presents the DC/DC power converter possible topologies. Section 3 describes the models that are used for the battery and super-capacitor storage elements. Sizing of the various system components and a performance comparison between classic and advanced Three Level (TL) DC/DC converters is detailed in section 4. Matlab/Simulink obtained simulations results are shown in Section 5. Finally, conclusions of the paper are given in section 6.

2. Topology description of the HESS and DC/DC converters

To improve the efficiency and performance of an EV or HEV vehicle, the HESS should satisfy the demands of high energy density, fast charging and discharging capabilities, long life cycle, low cost, and reduced size and volume. A lot of research has been investigated for varying the sources of energy sources in a HESS. One of the mostly used HESS is to combine batteries with super-capacitors. Several topologies were proposed in literature (Kuperman and Aharon, 2011). The proposed structure used in this paper is the parallel active hybrid topology shown in Figure 1 where each energy storage element is connected via a DC/DC power converter to a common DC-link. A unidirectional DC/DC converter is connected to the battery and a bidirectional DC/DC converter is used for the super-capacitor. This topology allows adapting the voltage level between the different storage elements and the electric vehicle system through DC/DC converters and enables the control of the energy and power flow on board the vehicle. This is the most sufficient configuration when comparing mass, volume and cost, as detailed in (Schaltz et al., 2007).

For the DC/DC converters, various topologies have been studied and published in several previous works (Lachichi and Schofield, 2006), (Yu and Lai, 2008), (Bouhalli et al., 2008). DC/DC converter topologies remain among the top concerns of researchers and industrials. The choice of a topology depends on its size, its energy efficiency, its cost and its ordering. Seven main topologies are most generally used: Boost, Buck, Buck/Boost, CUK and SEPIC (Du et al., 2010), Full Bridge (FB) (Schaltz et al., 2007), (Al Sakka et al., 2011) and Half Bridge (HB). Each structure has advantages and drawbacks. The boost and the buck/boost converters were basically proposed and examined for many HESS applications. These topologies are simple in use but have many drawbacks. For example, the boost converter suffers especially from elevated current and voltage ripples (Al Sakka et al., 2009), is characterized by large weight and volume and is unable to provide a high output voltage and has not the criteria of electrical isolation (Schaltz et al., 2007), (Al Sakka et al., 2011).

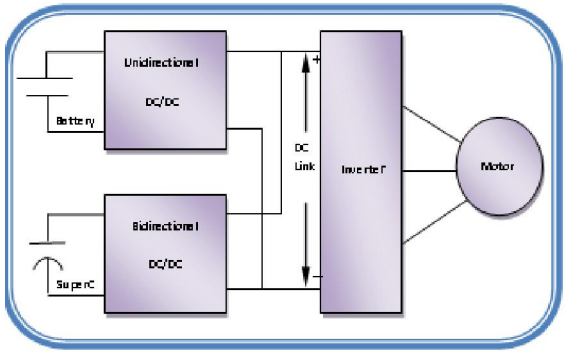

Figure 1. Parallel configuration HESS with 2 DC/DC converters

To tackle with the problems of classic converters, diverse new converter topologies (Schaltz et al., 2007), (Al Sakka et al., 2011), (Al Sakka et al., 2009) are proposed as alternatives. Recently, researchers and industrials have created new Three Level (TL) structures that represent good solution in applications with high input voltage and high switching frequency (Grbovic et al., 2010). In this case, the switchers are stressed on half of the total DC bus voltage. This enables for the use of lower-voltage-rated switches with better switching and conduction performance in comparison with switches rated on the full blocking voltage (Grbovic, 2009). Several studies ensured that the TL converter topology can be more efficient than many classic topologies (Du et al., 2010), (Ruan et al., 2008), (Cuzner et al., 2007) because of its reduced inductor size and its reduced switching frequency leading to reduced switch voltage stress and lower cost. For this reason, our study proposes to examine and compare two DC/DC converter topologies. Classic boost and buck/boost structures shown in Figure 2 are first examined, and then a TL topology shown in Figure 3 is studied. The comparison between the two converters topologies aims to sort for the more efficient converter topology that has more advantages and is better suitable for the HESS. Both structures are studied along with the sizing of all the constituting devices. Matlab/Simulink is then used to simulate and compare the behavior of the different topologies.

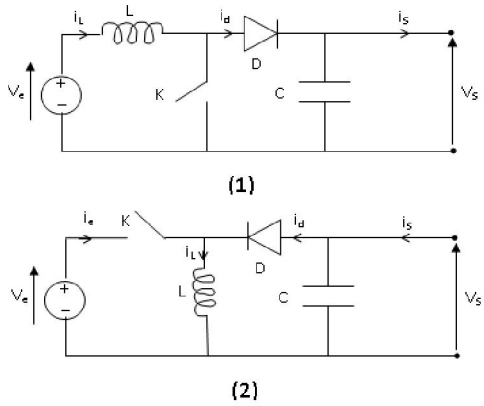

Figure 2. Classic DC/DC boost converter (1) and DC/DC buck/boost converter (2)

3. Energy storage models

HESSs, which include both batteries and super-capacitors, have been widely studied in HEV and EV applications (Lukic et al., 2008), (Lu et al., 2007), (Ozatay et al., 2004), (Anstrom et al. 2005), (Onoda and Emadi, 2004). The objective of integrating batteries and super-capacitors is to create an energy storage system with the high energy density attributes of a battery and the high power density of a super-capacitor. Moreover, Lithium-ion (Li-ion) batteries are increasingly used in several domains, due to their high voltage, high energy density, none memory effect and low self-discharge during storage. In this study, Li–ion batteries are selected as the battery source for the targeted HESS.

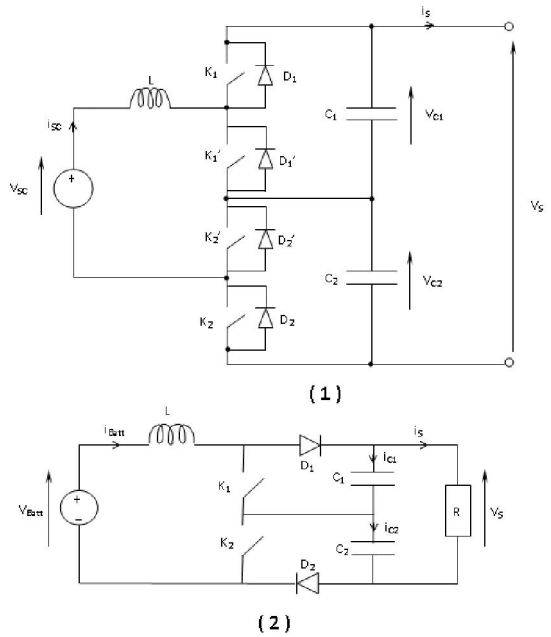

Figure 3. TL DC/DC buck/boost converter (1) and TL DC/DC boost converter (2)

3.1 Battery model

Various equivalent circuit models such as the R_{int} model, the R_C model or the Thevenin model are widely used in many EV studies (Pei et al., 2006), (Chiasson and Vairamohan, 2005). A good overview of the different available battery models is presented in (Singh and Nallanchakravarthula, 2005). The conventional model for a Li-ion battery consists of a voltage source that represents its internal voltage and a resistor representing its internal resistance (Tara et al., 2010), (Schaltz et al., 2009). In our study, we choose the Thevenin model, shown in Figure 4, due to its relative simplicity, its capability in modeling the dynamic and steady state behavior of the battery.

The electrical behaviour of the Thevenin model can be expressed by the following equations (1).

$$\begin{cases} \frac{U_{Th}}{dt} = -\frac{U_{Th}}{R_{Th}C_{Th}} + \frac{I_L}{C_{Th}} \\ U_L = U_{OC} - U_{Th} - I_L R_o \end{cases} \quad (1)$$

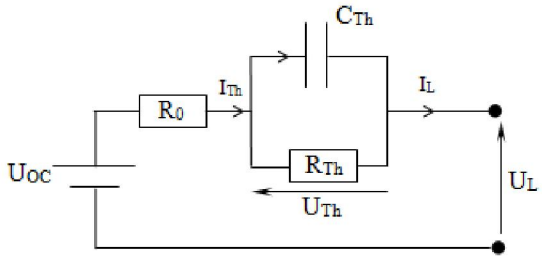

Figure 4. Schematic diagram for the Thevenin model

where U_{OC} denotes the open-circuit voltage. R_o and R_{Th} denote, respectively, the ohmic resistance and polarization resistance, representing the battery internal resistances. C_{Th} refers to the equivalent capacitance that is used to describe the transient response during charging and discharging. U_{Th} and I_{Th} denote the voltage and outflow current of C_{Th}, respectively.

3.2 Super-Capacitor model

Super-capacitors, as a distinct technology newly appearing in transportation domain, are power components well suited, for energy storage system of HEVs. Their lifetime is over 500,000 cycles and their power density (W/kg) is much higher than batteries. The super-capacitor can be stored with ten times more energy than conventional electrolytic capacitors. Their rapid development for vehicle applications is due to their power and life cycle characteristics that are significantly better in comparison with high power batteries.

In literature, two solutions are proposed to model the super-capacitor behavior. The first solution, based on the transmission-line model, proposes an equivalent circuit involving distributed capacitance C_i

and resistance R_i of the pores (Marie-Francoise et al., 2005). The second solution, proposed by Zubieta and Bonert (Zubieta and Bonert, 1998), describes the super-capacitor behavior by an equivalent electric circuit with two RC branches as shown in Figure 5 (1). The first branch is modeled as a voltage dependent differential capacitor C_1. It consists of a constant capacitor C_0 and a capacitor C_v whose value varies linearly with the voltage V_1 ($C_1 = C_0 + KV_1$). R_1 is the equivalent serial resistance. Compared with the first solution, the two branches model has a reduced complexity and requires shorter simulation time.

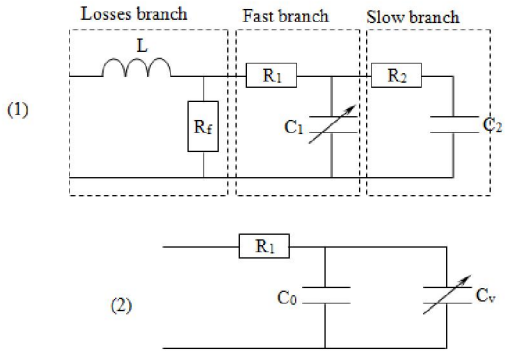

Figure 5. Equivalent circuit of super-capacitor with two branches model (1) and simplified model (2)

The R_1C_1 branch represents the main and fast branch that models the dominant charging and discharging behavior of the super-capacitor. This fast branch has a time range of few seconds. The R_2C_2 cell represents the slow branch with long time constants in the order of few minutes. The slow branch completes the fast one and is describes the internal energy distribution at the end of the super-capacitor charge or discharge. In many power electronic applications, super-capacitor is used to provide for a transient state peak power that may happen for few seconds. For such applications, the slow branch R_2C_2 can be neglected. In addition, the equivalent parallel resistance R_f can also be neglected during the fast charge/discharge of the super-capacitor because it represents the losses branch and has only impact on long-term storage performances (Marie-Francoise et al., 2005). For all these considerations, the obtained simplified equivalent model of the super-capacitor is shown in Figure 5 (2).

4. Sizing the different HESS components

The energy storage devices must be sized so that they store adequate energy (kWh) and supply sufficient peak power (kW) for the vehicle to provide the peak power needed for acceleration and regenerative braking according to the specified driving cycles (Burke, 2007). The storage power values are then used for determining the appropriate super-capacitor modules given their high power densities. However, the battery size is directly dependent on the vehicle energy requirements and on the average utilization factor of the selected technology. The energy utilization of any storage element cannot be 100 % because of many reasons such the number of load cycles, losses, constraints in the power converters etc. For example, the average energy utilization for batteries can be assumed to be 50%, and for super-capacitor to be 75%, roughly including the power electronics of the converters. According to the energy and the utilization factor values, the total mass of commercial battery modules are characterized and the number and structure of the battery and super-capacitor cells are determined to operate the system in a certain voltage range.

The different steps used for sizing the battery and super-capacitor storage sources are first detailed. In addition a comparison between two DC/DC converter topologies is presented. The first topology uses classic converters (boost for battery module and buck/boost for super-capacitors) as power interface and the second one uses TL DC/DC converter interfaces. The comparison of the two topologies will help choose for the most cost efficient structure as an interface between the energy sources and the DC bus. The system requirements are to operate 2 electric motors in front wheels having 850 kg weight, and a maximum speed of 130 km/h. 20 s are needed for the vehicle to accelerate from 0 to 100 km/h. The DC link voltage U_{DC} is of 400V.

4.1 Sizing the battery module

The battery is the main energy source of the system. Yet, it must be able to provide sufficient power to the vehicle so it rolls to a maximum speed of 130 km/h. In this case and according to the system specifications, the maximum instantaneous battery power is obtained P_{ch_batt} = 30 kW. We choose a SAFT Li-ion battery (Saft, 2012) designed for HEV with the following characteristics:

- Nominal voltage : 3.6 V
- Open circuit voltage : 4.0 V
- Average capacity (C/3) : 27 Ah
- Weight : 0.77 kg
- Volume : 0.38 l

The battery parameters are calculated according to the following equations.

- The total battery voltage

$$U_{batt} = (1 - \alpha)U_{DC} \quad (2)$$

Where α is the duty cycle, we choose α = 0.7 and $U_{DC} = 400V$.

- Series number of battery cells

$$N_{s\_batt} = \frac{U_{batt}}{V_{batt\_oc}} \quad (3)$$

- Total current delivered by the battery module

$$I_{tot-batt} = \frac{P_{ch\_batt}}{U_{batt}} \quad (4)$$

- Number of parallel branches

$$N_{p-batt} = \frac{I_{tot-batt}}{I_{batt-min}} \quad (5)$$

- Total number of battery cells

$$N_{tot-batt} = N_{p-batt} \times N_{s-batt} \quad (6)$$

- Total weight of the battery module

$$P_{tot-bat} = W_{batt} \times N_{tot-batt} \quad (7)$$

- Total volume of the battery module

$$V_{tot-bat} = V_{batt} \times N_{tot-batt} \quad (8)$$

- Total energy supplied by the batteries

$$E_{tot-batt} = N_{p-batt} \times C_{nom-batt} \times U_{tot-batt} \quad (9)$$

Where V_{batt_oc} and $I_{batt-min}$ denote the open circuit voltage and minimum current of the battery cell, respectively. W_{batt} refers to the weight and V_{batt} reresents the volume of battery cell. $U_{tot-batt}$ denotes the total nominal voltage delivered by series cells. Considering a nominal voltage of each battery cell equal to 3.6 V, the total voltage delivered by series cells is 108 V.

Using equations (2) to (9), the battery parameters are obtained as given in Table 1.

Table 1. Battery sized parameters

Parameter	Value
Voltage	120 V
Series cells	30
Total current	250 A
Parallel branches	4
Total energy	34.992 kWh

As shown in Table 1, the calculated total energy supplied by the batteries for an hour is equal to 34.992 kWh for 4 branches connected in parallel. However, the energy demanded by the vehicle and described in the set of specification is 30kWh. This difference is due to the integer value rounding errors obtained in the calculation of the number of the battery parallel branches. Actually, using equation (5), we got $N_{p-batt} = 3.33$, and in this case 4 branches are used.

4.2 Sizing of super-capacitors module

Super-capacitors are calculated to provide an acceleration of 100 km/h in t_a = 20 s and are obtained to have a maximum power P_{sc_max} = 45 kW. Super-capacitors are used to retrieve energy during the regenerative braking phases of the vehicle. Designing the super-capacitor module is based on determining the range of the operating voltage, the maximum transferred energy, and the number of elements in series and connected branches in parallel as shown by the following equations.

- The maximum transferred energy

$$E_{max-transf} = P_{sc-max} \times t_a \quad (10)$$

This maximum transferred energy is also related to the total number of super-capacitors and the range of the operating voltage per super-capacitor as follows:

$$E_{\max-transf} = \frac{1}{2} N_{tot-sc} \times C_{sc} \times (V_{ele-scmax}{}^2 - V_{ele-scmin}{}^2) \quad (11)$$

- Series super-capacitor number

$$N_{s-sc} = \frac{U_{sc-max}}{V_{ele-scmax}} \quad (12)$$

- Number of branches connected in parallel

$$N_{p-sc} = \frac{N_{tot-sc}}{N_{s-sc}} \quad (13)$$

- The total number of super-capacitor cells:

$$N_{tot-sc} = N_{s-sc} \times N_{p-sc} \quad (14)$$

- The instantaneous energy of the super-capacitors pack by Equation (15) :

$$E_{sc} = N_{p-sc} \times N_{s-sc} \times (\frac{1}{2} C_0 V_{ele-sc}{}^2 + \frac{1}{3} C_v V_{ele-sc}{}^3) \quad (15)$$

- Total capacity of the super-capacitors pack

$$C_{sc-tot} = C_{sc} \left(\frac{N_{p-sc}}{N_{s-sc}}\right) \quad (16)$$

- Equivalent internal resistance of the super-capacitors module

$$R_{sc-tot} = ESR \left(\frac{N_{s-sc}}{N_{p-sc}}\right) \quad (17)$$

Where ESR and C_{sc} denote the internal resistor and capacity of super-capacitor cell, respectively. $V_{ele-scmax}$ and $V_{ele-scmin}$ denote the maximum and minimum voltage per super-capacitor.

We chose the BCAP3000 (Boostcap, 2012) super-capacitor technology whose two branches model is given in (Lahyani et al., 2012). For $U_{DC} = 400V$, we choose $U_{sc-max} = 200\,V$. To get an acceptable efficiency, the minimum voltage is fixed to $U_{sc-min} = \frac{U_{sc-max}}{2}$. In this case, when the super-capacitors is discharged from U_{sc-max} and $\frac{U_{sc-max}}{2}$, 75% of the electric stored power is consumed.

From all these considerations and using equations (10) to (17), the parameters of the super-capacitor module are obtained in Table 2.

4.3 Classic Boost and buck/boost converters

In this section, classic Boost and buck/boost DC/DC converters shown in Figure 2 are considered. A unidirectional DC/DC converter is used to connect the battery to the DC Bus. However, a bidirectional DC/DC converter is needed to interface the super-capacitor module to the DC link. The chosen unidirectional converter allows increasing the battery output voltage in order to supply the DC Bus. In contrast, the reversible super-capacitor connected converter operates either in boost mode or in buck mode according to the need of the system. When the capacity of the super-capacitor is low, the power flows from the battery to charge the super-capacitor

without affecting the load current. During the start up and transient conditions, the battery, the super-capacitor or both of them will supply the load. In this case the converter will act as a boost converter to step up the super-capacitor output voltage to the DC Bus voltage (400V). When the power generated by the battery is more than the power needed for the load, the bidirectional converter which is connected to super-capacitor will act as a buck converter and charge the auxiliary power sources.

Table 2. Super-capacitor sized parameters

Parameter	Value
Transferred energy	900 kJ
Series cells	74
Parallel branches	2
Total capacity	81 F
Resistor	13.32 mΩ

Estimating the components of these two converters require the parameters calculation of the current smoothing inductance L and the filtering capacitor C (Figure 2). For the classic boost converter (Figure 2 (1)), the inductance and capacitance are given by Equation (18) and Equation (19):

$$L = \frac{U_{DC}}{4.f.\Delta I_{batt\_max}} \quad (18)$$

$$C = \frac{\alpha_{1max}.I_{1max}}{f.\Delta U_{DC\_max}} \quad (19)$$

Where ΔI_{batt_max} and ΔU_{DC_max} denote, respectively, the maximum current and maximum voltage ripples of the battery. f refers to the switching frequency. α_{1max} and I_{1max} denote the maximum duty cycle and maximum current, respectively.

For the buck/boost converter (Figure 2 (2)), the same Equation (19) is used for the capacitance, the inductance is obtained by Equation (20).

$$L = \frac{U_{DC}}{4.f.\Delta I_{sc\_max}} \quad (20)$$

Where ΔI_{sc_max} denotes the maximum super-capacitor current ripple.

The inductances and capacitances values for the classic boost and buck/boost converters are obtained as shown in Table 3. These parameters are obtained with ΔI_{batt_max} = 5A, ΔU_{DC_max} = 4V, ΔI_{sc_max} = 4.5A and a switching frequency fixed to 15 kHz.

Table 3. DC/DC classic converters sized parameters

Classic Boost Converter	Classic Buck/Boost converter
L = 1.33 mH	L = 1.48 mH
C = 1.125 mF	C = 1.25 mF

4.4 Sizing the TL converters

Sizing the TL converters requires the calculation the values of the current smoothing inductance L and the two filtering capacitors C_1 and C_2 as shown in Figure 4 (1).

For the Boost TL converter Figure 3 (2), the inductance and the capacities (C_1= C_2= C) are given by (21) and (22):

$$L = \frac{U_{batt}}{2\Delta I_{sc-max}f}.(2\alpha - 1) \quad (21)$$

$$C = \frac{2I_{scmax}(\alpha_{max}-0,5)}{\Delta U_{DC\_max}f} \quad (22)$$

For the Buck/Boost TL converter Figure 3 (1), the inductance and capacitors (C_1= C_2= C) values are given by (23) and (24).

$$L \geq \frac{U_{DC}}{16\Delta I_{sc-max}f} \quad (23)$$

$$C \geq max\left(\frac{I_{scmax}(1-\alpha_{min})}{2\Delta U_{DC\_max}f}, \frac{I_{scmax}(3-2\sqrt{2})}{2\Delta U_{DC\_max}f}\right) \quad (24)$$

Using the same voltage and current ripples and for the same switching frequency as for the classic converters, the inductance and filter capacities for the TL DC/DC converters are obtained in Table 4.

Table 4. DC/DC TL converters sized parameters

TL Boost converter	TL Buck/Boost converter
L = 0.32 mH	L = 0.37 mH
C = 1 mF	C = 0.56 mF

As shown in Table 3 and Table 4, the estimated inductance of the TL boost converter is approximately 25 % of the classic boost converter using the same value of current and voltage ripples and for the same switching frequency. The same phenomenon is observed while comparing the buck/boost classic and TL converters. In addition, the capacitors of the boost and buck/boost TL converters shown in Table 4 have also been reduced in comparison to those obtained for the classic converters given in Table 3.

Therefore, these reduced inductance and capacitor values of the TL topology allow reducing the cost, weight and volume of the converter. In comparison with the classic topology, the TL converter is more cost effective and allows for the best utilization of battery and super-capacitor technologies for both high energy and high power densities. In the next section, the two converter topologies are simulated to validate and confirm these results.

5. Simulation and results

In this section Matlab/Simulink is used to simulate the HESS system of Figure 1 integrating batteries, super-capacitors and the DC/DC converters.

Mathematical models of the different system components are implemented. In a first experiment, DC/DC converters are modeled in closed loop and are controlled by classic regulators (PI) to control the power flow from the hybrid energy storage sources to the DC load. The PI regulator is configured to control the deficiency of power and regulate the output voltage in addition to controlling the power sharing at the input side. In this first experiment the behaviour of the two converter topologies is simulated and the obtained results are compared.

The output voltage and the inductance current are obtained for a classic Boost converter (Figure 6 and Figure 7) and also for the TL Boost Converter (Figure 8 and Figure 9).

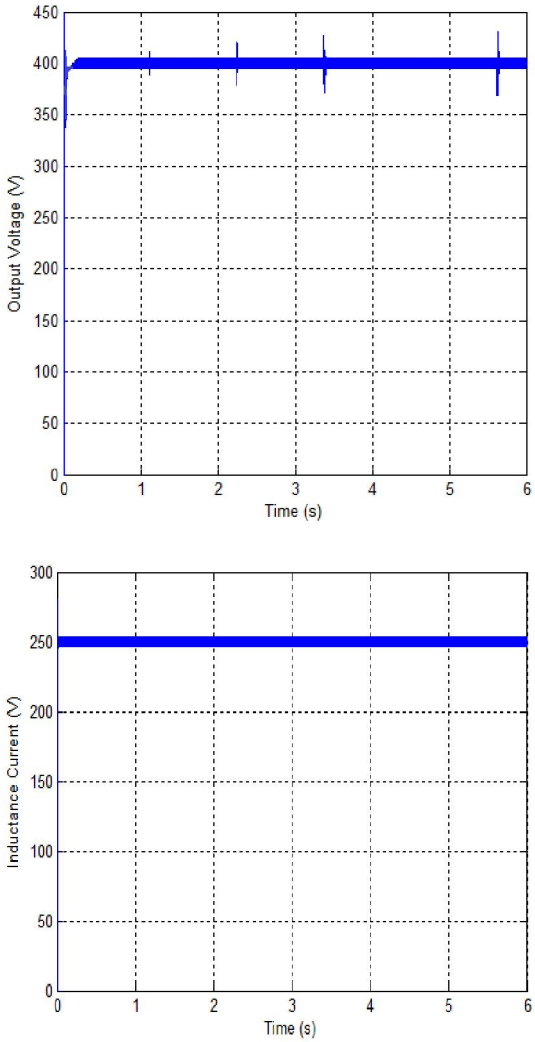

Figure 6. Output Voltage and Inductance Current of the Classic Boost Converter

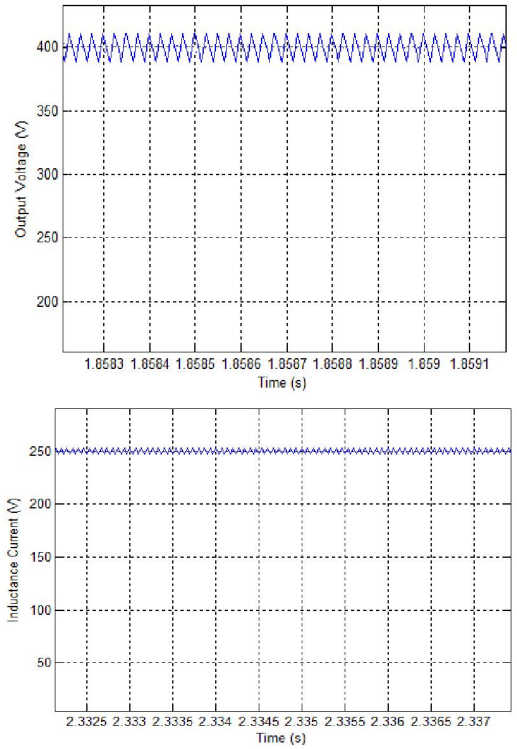

Figure 7. Output Voltage and Inductance Current ripples of the Classic Boost Converter

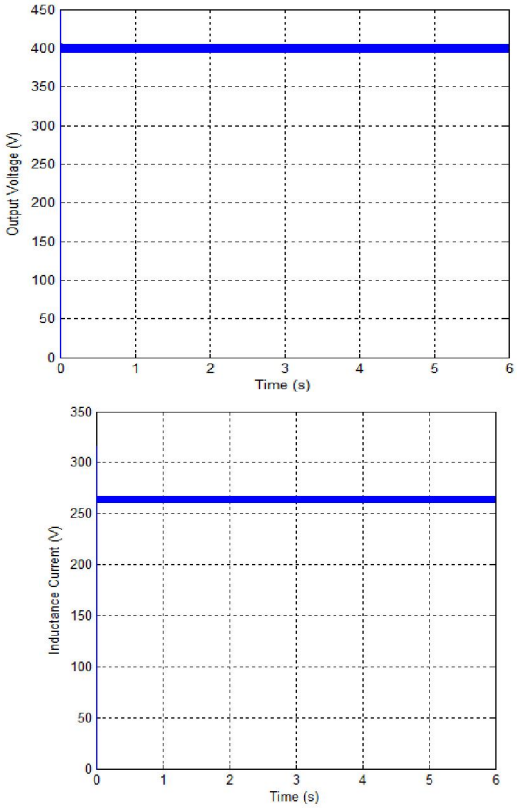

Figure 8. Output Voltage and Inductance Current of the Boost TL Converter

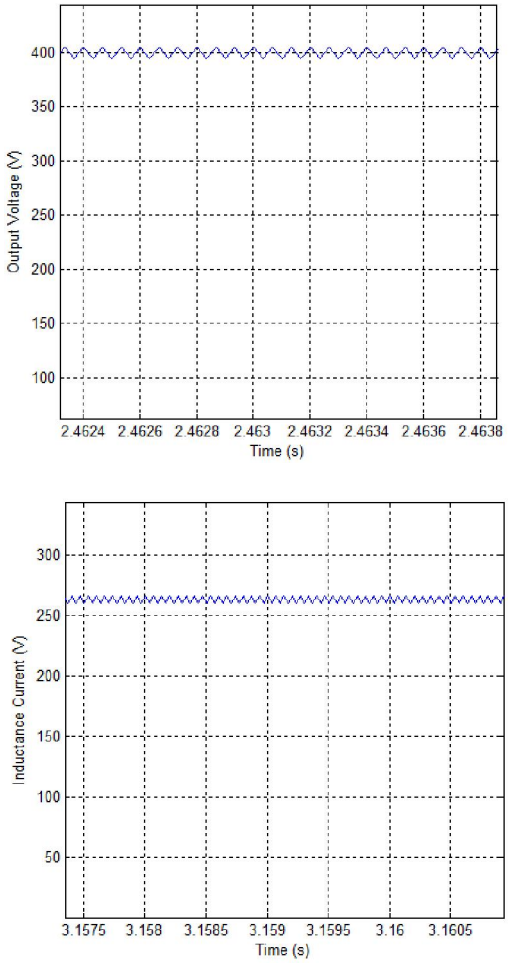

Figure 9. Output Voltage and Inductance Current Ripples of the Boost TL Converter

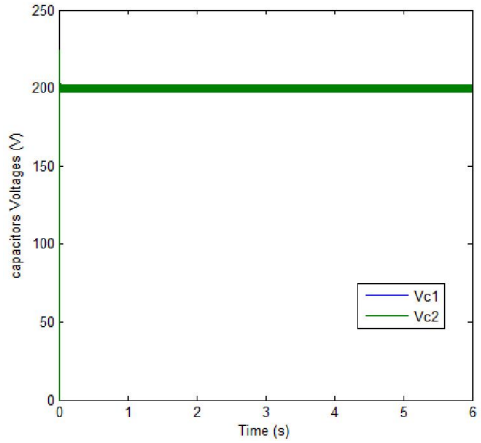

Figure 10. Capacitors voltages V_{c1} and V_{c2} with same values $C_1 = C_2 = 1$ mF

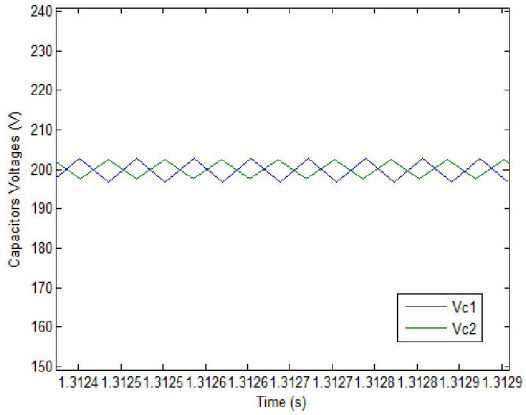

Figure 11. Voltages ripples of the two voltages V_{c1} and V_{c2}

Figure 10 clearly shows that the natural increase of the capacitor voltages V_{c1} and V_{c2} to a constant level (≈ 200V). These capacitors voltages remain well-balanced between them. Actually, if there are errors in the values of the capacitances, the voltage balancing is PI controlled and the system imposes average voltages with equal values. In Figure 11, the two capacitors voltages are shown to slightly oscillate around the 200V average value with ½ period out of phase between each capacitor voltage. The voltage ripple amplitude for the two capacitors is low, which explains the role of the boost TL converter described previously.

6. Conclusions

In this paper, we have presented and discussed the design case of an Hybrid Energy Storage System (HESS) for an Hybrid Electric Vehicle application. The HESS is composed by a pack of Li-ion battery and a pack of super-capacitors. The design methodology aims to find the optimal parameters of the different devices according to a proposed set of specifications. A comparison between two DC/DC converter topologies interfacing the HESS to the DC link is also performed. The studied topologies concern a classic DC/DC boost and buck/boost converters and a TL boost and buck/boost converters. The obtained results show that the TL converters enables for a reduced cost, weight and volume in the vehicle and allows for the best utilization of battery and super-capacitor technologies for both high energy and high power densities. Matlab/Simulink models of battery, super-capacitors and the different DC/DC converter topologies are implemented. The system behaviour and performance results are obtained and discussed. These obtained results confirm the design expectations and the cost efficiency of the TL topology.

Reference

1. Li Z, Onar O, Khaligh A. Design and Control of a Multiple Input DC/DC Converter for Battery/Ultra-capacitor Based Electric Vehicle Power System. 24th Annual IEEE APEC, 2009.
2. Lukic SM, Cao J, Bansal RC, Rodriguez F, Emadi A. Energy storage systems for automotive applications. IEEE Transactions Industrial Electronics 2008; 55 (6): 2258-2267.
3. Baisden AC, Emadi A. An ADVISOR based model of a battery and an ultra-capacitor energy source for hybrid electric vehicles. IEEE Transactions Vehicular Technology 2004;53(1): 199-205.
4. Cao J, Bharathan D, Emadi A. Efficiency and loss models for key electronic components of hybrid and plug-in hybrid electric vehicles' electrical propulsion systems. Proceedings of IEEE VPPC 2007: 477-482.
5. Kohler TP, Buecherl D, Herzog HG. Investigation of Control Strategies for Hybrid Energy Storage Systems in Hybrid Electric Vehicles. Proceedings of IEEE VPPC 2009: 1687-1693.
6. Hoelscher D, Skorcz A, Gao Y, Ehsani M. Hybridized Electric Energy Storage Systems for Hybrid Electric Vehicles. Proceedings of IEEE VPPC 2006: 1-6.
7. Miller JM, Deshpande U, Dougherty TJ, Bohn T. Power Electronic Enabled Active Hybrid Energy Storage System and its Economic Viability. 24th IEEE APEC 2009: 190–198.
8. Cao J, A Emadi A. New Battery/Ultra-Capacitor Hybrid Energy Storage System for Electric, Hybrid and Plug-in Hybrid Electric Vehicles. Proceedings of IEEE VPPC: Vehicle Power and Propulsion Conference 2009: 941-946.
9. Li R, Pottharst A, Fröhleke N, Böcker J. Energy storage scheme for rail-guided shuttle using ultracapacitor and battery. 11th International PEMC Conference 2004.
10. Li Z, Onar O, Khaligh A, Schaltz E. Design, control, and power Management of a battery/ ultra-capacitor hybrid system for small electric vehicles. In Proceedings SAE World Congress and Exhibition Detroit 2009.
11. Kuperman A, Aharon I. Battery–ultracapacitor hybrids for pulsed current loads: A review. Renewable and Sustainable Energy Reviews 2011; 15: 981–92.
12. Schaltz E, Andreasen SJ, Rasmussen PO. Design of propulsion system for a fuel cell vehicle. 12th European Conference on Power Electronics and Applications 2007: 1–10.
13. Lachichi A, Schofield N. Comparison of DC-DC Converter Interfaces for Fuel Cells in Electric Vehicle Applications. Proceedings of VPPC'06 IEEE Conference on Vehicle Power & Propulsion 2006: 1-6.
14. Yu W, Lai JS. Ultra High Efficiency Bidirectional DC-DC Converter with Multi-Frequency Pulse Width Modulation. Proceedings of APEC 23rd Annual IEEE Conference and Exposition on Applied Power Electronics 2008: 1079-1084.
15. Bouhalli N, Cousineau M, Sarraute E, Meynard T. Multiphase coupled converter models dedicated to transient response and output voltage regulation studies. Proceedings of EPE-PEMC 13th Conference on Power Electronics & Motion Control 2008: 281-287.
16. Du Y, Zhou X, Bai S, Lukic S, Huang A. Review of Non-isolated Bi-directional DC-DC Converters for Plug-in Hybrid Electric Vehicle Charge Station Application at Municipal Parking Decks. 25th Annual IEEE APEC: Applied Power Electronics Conference and Exposition 2010: 1145-1151.
17. Al Sakka M, Mierlo JV, Gualous H. DC/DC Converters for Electric Vehicles. Electric Vehicles – Modelling and simulations inTech Janeza Trdine 2011; 9: 309-332.
18. Al Sakka M, Mierlo JV, Gualous H, Culcu H. Thermal modeling and heat management of supercapaciotr modules for vehicle applications. Journal of Power Sources 2009; 194: 581-587.
19. Grbovi´c PJ, Delarue P, Le Moigne P, Bartholomeus P. A Bidirectional Three-Level DC–DC Converter for the Ultracapacitor Applications. IEEE Transactions Industrial Electronics 2010; 57(10): 3415-3430.
20. Grbovic PJ. High-voltage auxiliary power supply using series connected MOSFETs and floating self-driving technique. IEEE Transactions Industrial Electronics 2009; 56(5): 1446–1455.
21. Ruan X, Li B, Chen Q, Tan SC, Tse CK. Fundamental Considerations of Three-Level DC–DC Converters: Topologies, Analyses, and Control. IEEE Transactions on Circuits and Systems 2008; 55 (11): 3733-3743.
22. Cuzner RM, Bendre AR, Faill PJ, Semenov B. Implementation of a Non-Isolated Three Level DC/DC Converter Suitable for High Power Systems. IEEE Industry Applications Conference 2007:2001-2008.
23. Lu S, Corzine KA, Ferdowsi M. A New Battery/Ultracapacitor Energy Storage System Design and Its Motor Drive Integration for Hybrid Electric Vehicles. IEEE Transactions on Vehicular Technology 2007; 56 (4): 1516-1523.

24. Ozatay E, Zile B, Anstrom J, Brennan S. Power distribution control coordinating ultracapacitors and batteries for electric vehicles. Proceedings of the American Control Conference 2004;5: 4716–4721.
25. Anstrom JR, Zile B, Smith K, Hofmann H, Batra A. Simulation and field-testing of hybrid ultra-capacitor/battery energy storage systems for electric and hybrid-electric transit vehicles. 20th Annual IEEE APEC 2005;1:491–497.
26. Onoda S, Emadi A. PSIM-based modeling of automotive power systems: Conventional, electric, and hybrid electric vehicles. IEEE Transactions on Vehicular Technology 2004; 53 (2) :390–400.
27. Pei F, Zhao K, Luo Y, Huang X. Battery Variable Current-discharge Résistance Characteristics and State of Charge Estimation of Electric Vehicle. Proceedings of the 6th World Congress on Intelligent Control and Automation 2006.
28. Chiasson J, Vairamohan B. Estimating the state of charge of a battery. IEEE Transactions on Control Systems Technology 2005;13 (3):465-470.
29. Singh P, Nallanchakravarthula A. Fuzzy logic modeling of unmanned surface vehicle (USV) hybrid power system. Proceedings of the 13th International Conference on Intelligent Systems Application to Power Systems 2005.
30. Tara E, Shahidinejad S, Filizadeh S, Bibeau E, Battery Storage Sizing in a Retrofitted Plug-in Hybrid Electric Vehicle. IEEE Transactions on Vehicular Technology 2010; 59 (6): 2786-2794.
31. Schaltz E, Khaligh A, Rasmussen PO. Influence of battery/ ultracapacitor energy-storage sizing on battery lifetime in a fuel cell hybrid electric vehicle. IEEE Transactions on Vehicular Technology 2009; 58 (8): 3882–3891.
32. Marie-Francoise JN, Gualous H, Outbib R, Berthon A. 42V Power Net with supercapacitor and battery for automotive applications. Journal of Power Sources 2005; 143: 275–283.
33. Zubieta L, Bonert R. Characterization of double-layer capacitors for power electronics applications. IEEE-IAS 1998: 1149–1154.
34. Burke AF. Batteries and Ultracapacitors for Electric, Hybrid, and Fuel Cell Vehicles. Proceedings of the IEEE 2007; 95 (4): 806-820.
35. The Saft website. Available online; February 2012 [accessed on February 2012]. http://www.saftbatteries.com/doc/Documents/liion/Cube572/54042_VLM_cells_0305.d0d8d859-9174-42f2-84b2-19632e4b0760.pdf.
36. Datasheet BOOSTCAP Ultracapacitor. Available online; February 2012 [accessed on February 2012]. http://www.tecategroup.com/capacitors/datasheets/maxwell/K2_series.pdf.
37. Lahyani A, Venet P, Troudi A, Guermazi A. Control Strategy for Optimal Combination of Supercapacitors and Battery in 500 kVA rated UPS. International Journal of Electrical and Electronics Engineering. IJEEE WASET 2012.

7/19/2014